Schottky barrier height tuning of silicides on p-type Si (100) by aluminum implantation and pulsed excimer laser anneal

Shao-Ming Koh,[1] Xincai Wang,[2] Thirumal Thanigaivelan,[3] Todd Henry,[3] Yuri Erokhin,[3] Ganesh S. Samudra,[1] and Yee-Chia Yeo[1,a)]
[1]*Department of Electrical and Computer Engineering, National University of Singapore, 10 Kent Ridge Crescent, 119260, Singapore*
[2]*Singapore Institute of Manufacturing Technology, A*STAR (Agency for Science, Technology and Research), 3 Research Link, 117602, Singapore*
[3]*Varian Semiconductor, 35 Dory Road, Gloucester, Massachusetts 01930, USA*

(Received 11 May 2011; accepted 23 August 2011; published online 6 October 2011)

We investigate the tuning of Schottky barrier height (SBH) of nickel silicide formed by pulsed excimer laser anneal of nickel on silicon implanted with aluminum (Al). A wide range of laser fluence was investigated, and it has been found that laser fluence influences the distribution of Al within the silicide and at the silicide/silicon interface. This in turn affects the effective whole SBH ($\Phi_B{}^p$) at the silicide/silicon junction. High Al concentration at the silicide/silicon interface and high temperature for nano-second duration to achieve Al activation while keeping the Al concentration within the silicide low is vital for achieving low $\Phi_B{}^p$. We demonstrate the achievement of one of the lowest reported $\Phi_B{}^p$ of ~0.11 eV. This introduces a new option for forming nickel silicide contacts with reduced contact resistance at low thermal budget for possible adoption in future metal-oxide-semiconductor transistor technologies. © *2011 American Institute of Physics*. [doi:10.1063/1.3645018]

I. INTRODUCTION

Nickel silicide (NiSi) is the current salicide material used in mainstream complementary metal-oxide-semiconductor (CMOS) industry. However, the metal Fermi level of NiSi at the NiSi/Si (100) interface is such that a Schottky barrier height (SBH) of ~0.67 eV for electrons and ~0.4 eV for holes are obtained for n-Si and *p*-Si, respectively.[1,2] The silicide contact resistance (R_C) is an exponential function of SBH, and a large SBH leads to a large R_C. High R_C has been identified as one of the bottlenecks for achieving continual improvement of speed performance in the scaling of field-effect transistor (FET) technology.[3–5] Much research efforts have been devoted to reducing the SBH through exploration of novel silicide materials and their integration,[6–11] as well as dopants[1,2] or impurities[12–22] segregation at the NiSi/Si interface. In the aforementioned work, the metal silicides were formed by conventional rapid thermal anneal (RTA). With scaling of device geometry into the nanoscale regime, the integration of NiSi in CMOS devices with aggressively scaled ultra shallow junction faces reliability issues.[23,24] Increase in drain leakage current can result from diffusion of Ni atoms to the drain-channel p-n junction to form generation-recombination centers[25,26] and from silicide piping in the p-n junction under the gate caused by phase transition from NiSi to nickel disilicide ($NiSi_2$).[27–29] Hence, the formation of metal silicides with low thermal budget that can overcome these scaling issues and that can reduce contact resistance is of utmost importance.

Recently, there has been a renewed interest in using laser annealing (LA) as an alternative to conventional RTA for silicide formation.[24,30,31] The duration of a laser pulse can be as short as several tens of nanoseconds, so that the total thermal budget incurred during LA is low. Irradiation of a metal film on silicon with laser thus allows the formation of a metal silicide at low thermal budget. This can help to suppress nickel diffusion and nickel silicide agglomeration.[24,30–32] While silicide formation using LA[24,30–39] has been experimentally demonstrated, little, if any, experimental work has been done to understand SBH modulation at the silicide/silicon interface with dopant incorporation for silicides formed by LA. It has been demonstrated recently that SBH of NiSi on *p*-Si can be reduced by aluminum (Al) ion implantation and its segregation after Ni deposition and silicidation with RTA, achieving a low hole SBH ($\Phi_B{}^p$) of 0.12 eV.[12–15]

In this work, we present a systematic investigation of Al distribution after Ni silicidation with a pulsed laser anneal (PLA). Here we focus on the dependence of the Al profile within the NiSi and at the NiSi/Si interface on the pulsed laser fluences and its impact on $\Phi_B{}^p$ modulation. We demonstrate that an optimum combination of Al segregation and PLA to form NiSi is effective in lowering the $\Phi_B{}^p$, achieving one of the lowest reported $\Phi_B{}^p$ of 0.11 eV.

II. EXPERIMENT

Wet thermal oxidation was performed on p-type Si (100) wafers (4–8 Ω cm) to form a 200 nm thick SiO_2. The SiO_2 was patterned and etched to define active areas. Next, Al ion implantation with doses ranging from 5×10^{13} cm^{-2} to 10^{16} cm^{-2} was carried out at 1.5 keV. The projected Al ion range and straggle are estimated to be ~50 Å and ~26 Å,

a)Author to whom correspondence should be addressed. Electronic addresses: yeo@ieee.org and eleyeoyc@nus.edu.sg.

respectively, using simulation.[40] After removal of native oxide in the active region [using dilute hydrofluoric acid solution HF:H_2O (1:100) for 120 s], 7 nm thick Ni film was then sputter-deposited prior to PLA for silicide formation [Fig. 1(a)]. Laser annealing was carried out using a 248 nm KrF excimer laser with full-width half-maximum pulse duration of 23 ns in N_2 ambient. The laser anneal employed a single pulse of homogenized laser beam irradiating a 2×2 mm^2 area in each exposure with fluences ranging from 200 mJ/cm^2 to 700 mJ/cm^2. The laser beam exposure was stepped to cover whole sample with an overlap of 2.5% between each step. Excess Ni was selectively removed with a sulfuric acid-peroxide solution H_2SO_4:H_2O_2 [4:1] at a temperature of 120|°C for 120 s. Finally, aluminum was deposited on the backside of the wafer to form an ohmic contact.

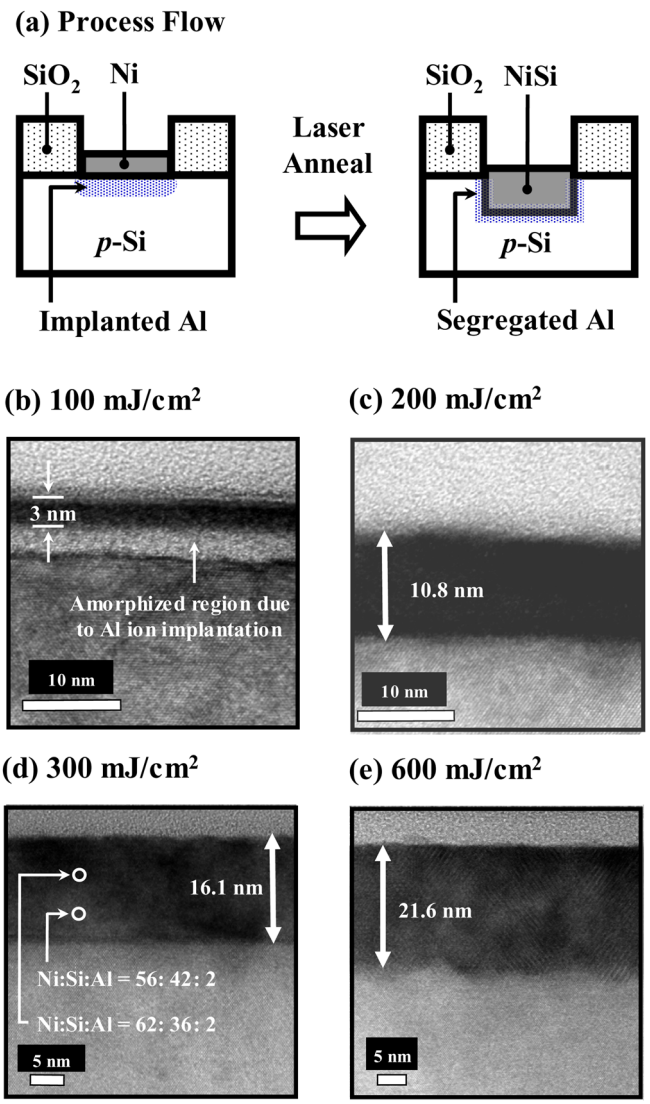

FIG. 1. (Color online) (a) Schematics illustrating the process flow used for fabricating contact structures comprising NiSi on p-type Si. The contact structures received Al implant prior to nickel silicidation using a pulsed laser anneal (PLA). Silicidation was performed in the 100 μm $\times$ 100 μm square-shaped active regions defined by the SiO_2. TEM images of NiSi formed after PLA of (b) 100 mJ/cm^2, (c) 200 mJ/cm^2, (d) 300 mJ/cm^2, and (e) 600 mJ/cm^2 reveal atomically flat NiSi/Si interface. The thickness of silicide formed with pulsed laser anneal increases with increasing laser fluence.

III. SBH MODULATION WITH ALUMINUM IMPLANT AND LASER-ANNEAL FOR SILICIDE FORMATION

Transmission electron microscopy (TEM) images of different samples after silicidation with PLA are shown in Figs. 1(b) to 1(e). In Figs. 1(b) to 1(e), an Al dose of 1×10^{16} cm^{-2} was implanted at 1.5 keV into each sample prior to Ni deposition and silicidation. It should be noted that the Al-implanted region was amorphized to a depth of ~6 nm. With a laser fluence of 100 mJ/cm^2, a 3 nm thick nickel silicide was formed, and an underlying amorphous region could still be visible [Fig. 1(b)]. With increasing laser fluence, the nickel silicidation covers a greater depth and a thicker NiSi is formed. At 200 mJ/cm^2, a ~11 nm thick nickel silicide is formed, completely consuming the amorphized region due to the Al implant. High resolution TEM images also reveal an atomically flat and sharp silicide/Si interface for samples irradiated with laser fluences of 200 mJ/cm^2 and above. Although a high Al dose was introduced by implant, no Al spiking is observed after silicidation. Energy dispersive x-ray (EDX) analysis of the sample irradiated with a laser fluence of 300 mJ/cm^2 shows a Ni-rich nickel silicide layer at the top [Fig. 1(c)]. The Ni to Si ratio reduces as one moves toward the silicide/Si interface. The fast heating and quenching of the film in nanoseconds during the laser anneal prevents the redistribution of the atoms within the heated region, hence resulting in a graded Ni-Si profile within the silicide.[39]

To investigate the impact of Al incorporation and PLA on Φ_B^p of the nickel silicide formed, current-voltage (I-V) curves of Schottky diodes with Al ion implantation (1×10^{16} cm^{-2} at 1.5 keV) and silicided with different laser fluences were measured (Fig. 2). The I-V plot of the sample with no Al ion implantation and silicided using RTA at 450 °C 30 s is also included as a reference. With increase in laser fluence, the reverse current increases, indicating a reduction in Φ_B^p. To evaluate the degree of rectification in the I-V characteristics, a rectification ratio R_r is used. R_r is defined as

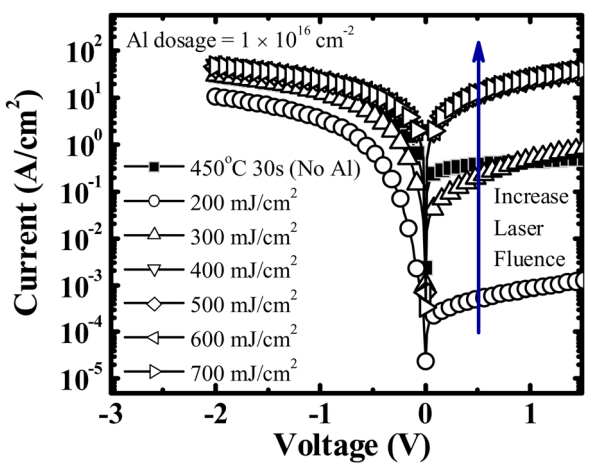

FIG. 2. (Color online) I-V characteristics of nickel silicide contact structures formed by pulsed laser annealing of Al-implanted p-type Si. Various laser fluences ranging from 200 to 700 mJ/cm2 were used. A reference sample that received no Al implant and that was nickel-silicided using RTA at 450 °C 30 s is also included for comparison. For nickel silicides formed by laser anneal, the I-V curves show less rectifying characteristics with increasing laser fluence.

the ratio of the forward current taken at a forward voltage of −1 V to the reverse current taken at a reverse voltage of 1 V. An ohmic contact has a R_r close to 1 while a higher $\Phi_B{}^p$ leads to a higher R_r. The R_r for the reference sample is ~32. With a laser fluence of 200 mJ/cm^2, the Al-implanted nickel silicide contact formed on *p*-Si is highly rectifying with R_r of $\sim 4.24 \times 10^3$. With a laser fluence of 700 mJ/cm^2, the Al-implanted nickel silicide contact formed on *p*-Si has an *I-V* characteristics approaching that of an ohmic contact with R_r of ~1.

As the *I-V* behaviors of samples annealed at laser fluences of 300 mJ/cm^2 and below are different from those annealed at laser fluences above 300 mJ/cm^2, we will discuss the results separately. In the following discussion, we will categorize laser fluences at 300 mJ/cm^2 and below as low energy laser fluence and laser fluences above 300 mJ/cm^2 as high energy laser fluence.

A. SBH modulation with Al implant and silicidation using high laser fluence

Two important observations have been made so far: in comparison to the reference NiSi/*p*-Si sample, (1) silicidation of Al-implanted sample using high laser fluence results in an increase in the reverse bias hole current, indicating a decrease in $\Phi_B{}^p$, and (2) reducing the laser fluence to below 300 mJ/cm^2 results in a more rectifying *I-V* behavior, indicating an increase in $\Phi_B{}^p$. In this section, we will discuss physical mechanism behind the first observation.

To understand the distribution of the Al in the samples after PLA, time-of-flight secondary-ion-mass spectroscopy (TOF-SIMS) analysis for samples irradiated with laser fluences of 500 mJ/cm^2 and 700 mJ/cm^2 is carried out (Fig. 3). SIMS analysis reveals the segregation of Al near the silicide/Si interface for samples annealed at laser fluences of 500 mJ/cm^2 and 700 mJ/cm^2. Simulation of laser interaction with material (SLIM)[41] was carried out to estimate the maximum temperature experienced by the samples during laser irradiation. Simulations predict that the temperatures of the samples irradiated with 500 mJ/cm^2 and 700 mJ/cm^2 could be as high as ~1750 K and ~1820 K, respectively. Using the pre-

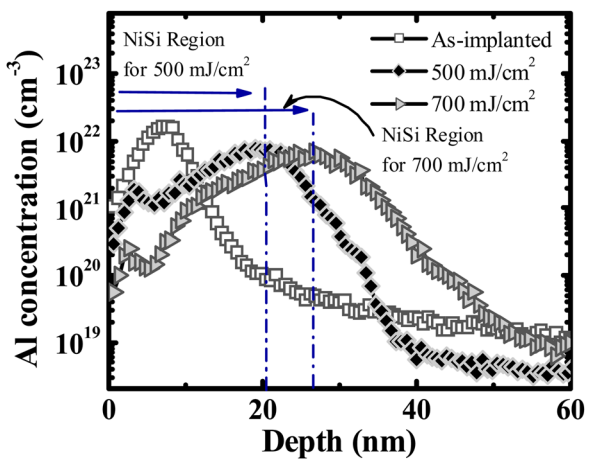

FIG. 3. (Color online) TOF-SIMS profiles of Al after Ni deposition and silicidation at a laser fluence of 500 mJ/cm^2 and 700 mJ/cm^2. Al segregation near the interface between nickel silicide and Si could be observed.

exponential factor D_o of 4.73 cm^2/s and activation energy E_A of 3.35 eV,[42] the diffusion lengths of Al under the PLA with laser fluences of 500 mJ/cm^2 and 700 mJ/cm^2 were calculated to be ~0.1 nm and ~0.15 nm, respectively, suggesting that solid state diffusion cannot be used to fully explain the large distance traveled by Al atoms for such a short annealing duration. As the melting temperatures of Ni and crystalline Si are 1728 K and 1685 K, respectively,[43] and amorphous silicon has a melting temperature of approximately 300 K lower than crystalline silicon,[44] it is likely that PLA with laser fluence of 500 mJ/cm^2 and 700 mJ/cm^2 could have caused complete melting of the Ni film as well as the underlying Al-implanted Si region. In a melt phase, the diffusion coefficient of an atom can reach five to eight orders in magnitude higher than that in solid,[45] thus allowing the Al atoms to redistribute over a larger distance.

It is well reported that silicide films tend to nucleate and form island to minimize the surface, grain-boundary and interface energy when high temperature is used for silicide formation with conventional RTA. In addition, agglomeration is likely to occur at a lower temperature with reduced films thicknesses as its occurrence is highly dependent on the ratio of the silicide grain size to the as-deposited film thickness.[46,47] However, no agglomeration is observed for silicides formed using PLA despite the high temperature used. It is believed that the fast heating and quenching of the film in nanoseconds does not leave sufficient time for agglomeration to happen.

Next, characterization of the activation energy[48] associated with carrier transport across the contact was carried out by varying the measurement temperature from 180 K to 280 K. This would measure the small $\Phi_B{}^p$ for diodes irradiated with laser fluences above 300 mJ/cm^2. Arrhenius plots with different forward voltages and linear fitting for various curves in the low temperature regime are used to extract the $\Phi_B{}^p$ for samples annealed at the laser fluence of 500 mJ/cm^2 [Fig. 4(a)] and 700 mJ/cm^2 [Fig. 4(b)]. The average value of $\Phi_B{}^p$ extracted for sample irradiated with 500 mJ/cm^2 and 700 mJ/cm^2 is ~0.15 eV and ~0.11 eV, respectively. First principles calculations for NiSi/Si interface showed that the most stable configuration (lowest energy state) of certain ion-implanted species is at the substitutional site in the Si lattice in the first few monolayers from the silicide/Si interface after low temperature thermal annealing.[49] The Al atoms may also reside at the subsitutional sites in Si near the silicide/Si interface, allowing them to behave as acceptors in Si. In addition, recognizing that PLA is an non-equilibrium process, the rapid melt resolidification rate could incorporate Al atoms at substitutional sites in concentrations that greatly exceed their maximum solid solubility.[50,51] Al doping is known to create an acceptor-type trap level at 0.067 eV above the valence band.[48] The Al trap states at the interface is expected to become fully ionized (negatively charged) due to the band bending caused by the workfunction difference between the metal silicide and Si. As a result, the charged Al atoms at the interface will introduce an electrical dipole at the NiSi/Si interface, causing an increase in band bending of the silicon valence band and a decrease in the barrier depletion width [Fig. 4(c)]. The narrowing of the barrier depletion width will lead to the lowering of effective $\Phi_B{}^p$.

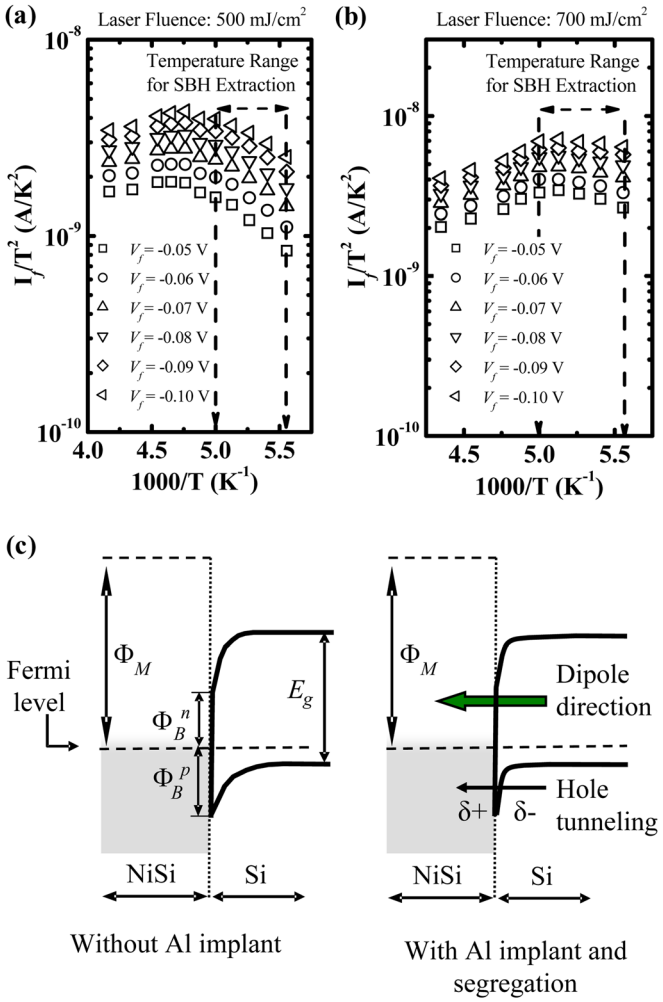

FIG. 4. (Color online) Measurements for extraction of $\Phi_B{}^p$ of NiSi on *p*-Si. The slope of the linear fit of the curves in the low temperature regime is used to extract the $\Phi_B{}^p$ for samples irradiated at laser fluence of (a) 500 mJ/cm^2 and (b) 700 mJ/cm^2. The *p*-Si samples were implanted with an Al dose of 10^{16} cm^{-2} at 1.5 keV. (c) The presence of negatively charged Al on the Si side of the silicide/Si interface could result in the narrowing of the depletion width for enhanced hole tunneling.

Figure 5 plots the extracted $\Phi_B{}^p$ as a function of the integrated interface dose of Al for samples annealed at laser fluence of 500 mJ/cm^2 and 700 mJ/cm^2. The integrated interfacial dose of Al is defined to be the dose of Al in the Si region within 5 nm from the silicide/Si interface. It is interesting to note that while the sample irradiated at the laser fluence of 700 mJ/cm^2 has a lower integrated interface Al dose as compared to the sample irradiated at the laser fluence of 500 mJ/cm^2, a lower $\Phi_B{}^p$ is extracted. The higher laser fluence (and hence higher annealing temperature) could have resulted in improved activation (i.e., larger percentage of Al atoms residing in the substitutional sites of Si at the silicide/Si interface).

B. SBH modulation with Al Implant and silicidation using low laser fluence

Next, the decrease in reverse bias hole current for diodes irradiated with laser fluences below 300 mJ/cm^2 is investigated. To investigate the increase in $\Phi_B{}^p$ with Al incorporation and silicidation at low laser fluence, the depth profile of Al in NiSi/*p*-Si is examined using the TOF-SIMS for the sample irradiated with laser fluence of 200 mJ/cm^2 (Fig. 6). Figure 6 reveals a high concentration of Al within the bulk of the silicide. SIMS analysis shows that Al concentration within the silicide for samples annealed at laser fluence of 200 mJ/cm^2 is much higher when compared to the sample irradiated at 500 mJ/cm^2 and 700 mJ/cm^2. In addition, Al atoms for the sample annealed at 200 mJ/cm^2 experience less diffusion as compared to samples irradiated at 500 mJ/cm^2 or 700 mJ/cm^2. SLIM simulation shows that the maximum temperature generated in the sample irradiated at 200 mJ/cm^2 is ~890 K. By comparing these phenomena, we believe that when PLA at low laser fluence with temperature below the melting threshold of the sample, interdiffusion of elements at the Ni and Si interface occurs through a solid state reaction.

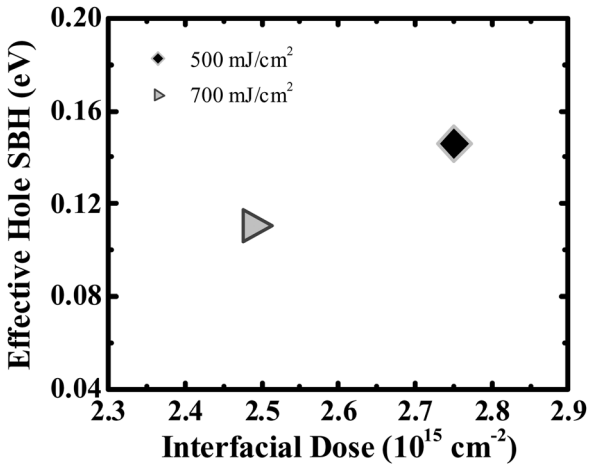

FIG. 5. $\Phi_B{}^p$ as a function of integrated interfacial dose of Al. Integrated interface dose of Al is extracted by integrating the Al concentration profiles in the Si region within 5 nm from the silicide/Si interface.

Further investigation is carried out by comparing the *I-V* curves of Schottky diodes with different Al implant doses and silicided using a fixed laser fluence of 200 mJ/cm^2 [Fig. 7].

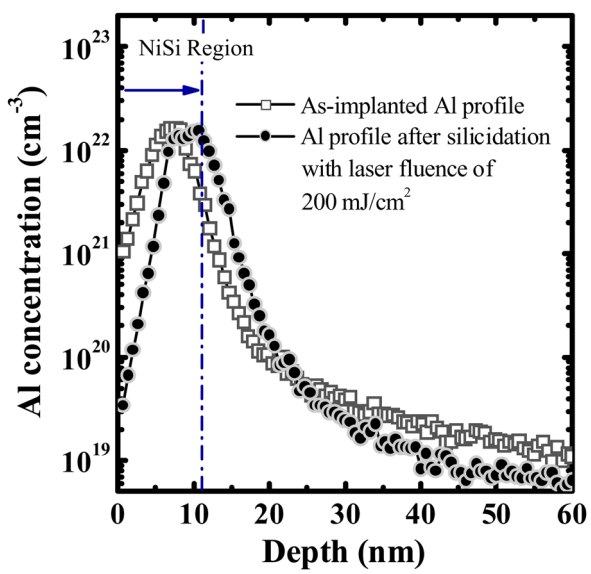

FIG. 6. (Color online) TOF-SIMS profile of Al after Ni deposition and silicidation at laser fluence of 200 mJ/cm^2, as well as the as-implanted Al profile (in silicon).

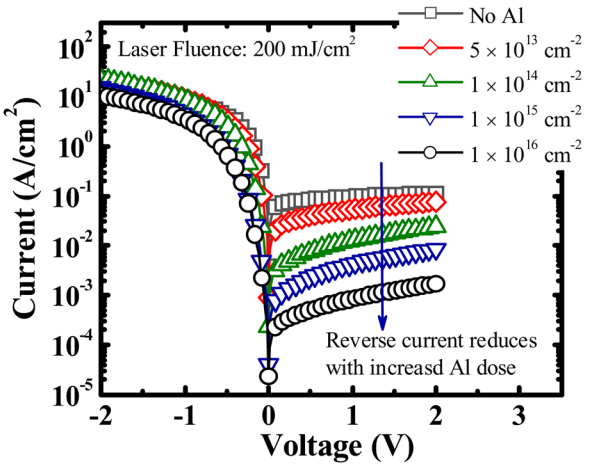

FIG. 7. (Color online) *I-V* characteristics of samples with various Al doses ranging from 0 to 10^{16} cm^{-2} and silicided at a fixed laser fluence of 200 mJ/cm^2. The rectifying *I-V* behavior of NiSi increases with aluminum ion implantation dose.

The reverse bias hole current reduces with an increase in Al implant dose. Taking series resistance and non-ideality factor into consideration, the $\Phi_B{}^p$ extracted from the *I-V* curves are summarized in Fig. 8(a). The $\Phi_B{}^p$ values are determined by fitting the *I-V* characteristics of the Schottky diode using:

$$I = A^* A T^2 \exp\left(-\frac{q\phi_B^p}{k_B T}\right)\left[1 - \exp\left(\frac{-q(V - IR)}{nk_B T}\right)\right], \quad (1)$$

where A^* is the Richardson constant for thermionic emission, A is the diode area, T is the temperature, q is the electronic charge, k_B is the Boltzmann's constant, n is the non-ideality factor, and R is the series resistance. The n and R are determined using[52]

$$\frac{d|V_F|}{d(\ln(|I_F|))} = n\frac{k_B T}{q} + |I_f|R, \quad (2)$$

where V_F and I_F are the forward voltage and current, respectively. It is observed that increasing the Al dose increases the $\Phi_B{}^p$ of NiSi from ~0.46 eV for sample without Al implant to ~0.59 eV for sample with 10^{16} cm^{-2} dose of Al implant, representing a 28% increase in $\Phi_B{}^p$.

One point to note is that the instantaneous temperature during laser irradiation at low laser fluence may result in little or lesser Al activation at the silicide/Si interface as compared to those annealed at high laser fluences that were discussed in the previous section. This implies that the impact of the Al at the silicide/Si interface on SBH reduction for samples annealed at 200 mJ/cm^2 may be much lesser in comparison to samples anneal at 400 mJ/cm^2 and higher. The increment of the $\Phi_B{}^p$ with the amount of Al incorporation suggests that the presence of Al within the silicides is likely to be responsible for the increase in $\Phi_B{}^p$. The observed phenomenon of $\Phi_B{}^p$ tuning with Al incorporation within the silicides is consistent with other reported literatures where Al is introduced into the metal silicide either by co-sputtering[9–11] or ion implantation.[6,8] The underlying physics is believed to be due to the incorporation of Al, which has a

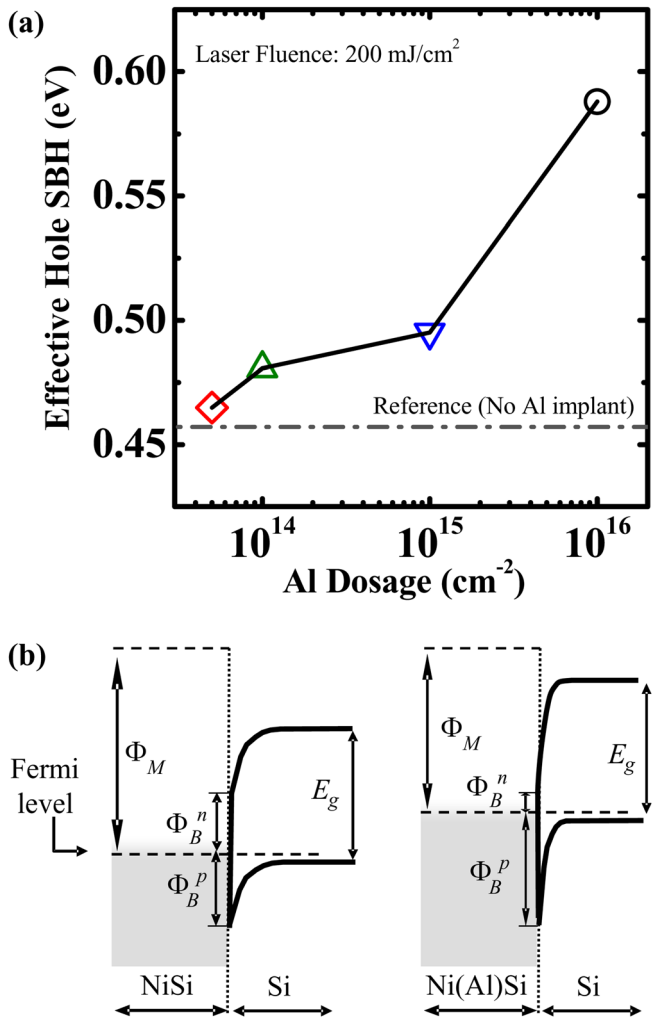

FIG. 8. (Color online) (a) Comparison of the average $\Phi_B{}^p$ as a function of Al implantation dose. For each split, 5 samples were measured. (b) Schematic depicting the energy-band diagram of NiSi/Si junctions with and without Al incorporation. Presence of Al within metal silicide is believed to have tuned the intrinsic workfunction of the metal silicide, leading to an increase in $\Phi_B{}^p$.

lower workfunction as compared to NiSi, resulting in a reduction in the intrinsic workfunction of NiSi,[9–11] as illustrated in Fig. 8(b). Assuming that the sum of hole and electron SBH is equal to the bandgap of Si, the movement of the Fermi level of silicide toward the conduction bandedge of Si with increase in Al incorporation will result in an increase in $\Phi_B{}^p$ and a decrease in electron SBH. It has been suggested that the introduction of hydrogen during metal sputtering may passivate defects localized at the metal-semiconductor influence, and hence influencing the SBH.[53] However, it should be noted that the samples in this work were subjected to subsequent high temperature annealing during silicidation, which is likely to remove any hydrogen introduced during sputtering.[53,54] In addition, the change in SBH (observed in this work) with the amount of Al incorporation is indicative that the presence of Al plays a role in SBH modulation.

IV. CONCLUSION

In summary, we have demonstrated tuning of the SBH of NiSi on *p*-Si by Al ion implantation and PLA. Findings

show that laser fluence influences the distribution and perhaps activation of Al, which in turn affects $\Phi_B{}^p$ modulation at the silicide/silicon junction. The results indicate that Al ion implantation and PLA to form NiSi could be applied to form NiSi contacts with reduced contact resistance for future technology generations.

ACKNOWLEDGMENTS

We acknowledge research grant (Award No. NRF-RF2008-09) from the National Research Foundation (NRF), Singapore. S.-M. Koh thanks Globalfoundries Singapore Pte Ltd. and the Economic Development Board (EDB) of Singapore for a Graduate Scholarship.

[1]Z. Qiu, Z. Zhang, M. Ostling, and S.-L. Zhang, IEEE Trans. Electron Devices **55**(1), 396 (2008).
[2]Z. Zhang, Z. Qiu, R. Liu, M. Ostling, and S.-L. Zhang, IEEE Electron Device Lett. **28**, 565 (2007).
[3]ITRS International Technology Roadmap for Semiconductors, http://public.itrs.net/ (See pages 2–5 of the Process Integration, Devices and Structures chapter of the ITRS 2009 Edition for information about the challenges critical to sustaining historical scaling of CMOS technology as per Moore's Law).
[4]S. D. Kim, C. M. Park, and J. C. S. Woo, IEEE Trans. Electron Devices **49**(3), 467 (2002).
[5]A. Dixit, A. Kottantharayil, N. Collaert, M. Goodwin, M. Jurczak, and K. D. Meyer, IEEE Trans. Electron Devices **52**(6), 1132 (2005).
[6]I. Ok, C. D. Young, W. Y. Loh, T. Ngai, S. Lian, J. Oh, M. P. Rodgers, S. Bennett, H. O. Stamper, D. L. Franca, S. Lin, K. Akarvardar, C. Smith, C. Hobbs, P. Kirsch, and R. Jammy, Dig. Tech. Pap. - Symp. VLSI Technol. **17** (2010).
[7]S.-M. Koh, W.-J. Zhou, R. T.-P. Lee, M. Sinha, C.-M. Ng, Z. Zhao, H. Maynard, N. Variam, Y. Erokhin, G. S. Samudra, and Y.-C. Yeo, Electrochem. Soc. Trans. **25**(7), 211 (2009).
[8]H. Fukutome, K. Okabe, K. Okubo, H. Minakata, Y. Morisaki, K. Ikeda, T. Yamamoto, K. Hosaka, Y. Momiyama, M. Kasa, and S. Satoh, Tech. Dig. – Int. Electron Devices Meet. **59** (2008).
[9]A. T.-Y. Koh, R. T.-P. Lee, A. E.-J. Lim, D. M.-Y. Lai, D.-Z. Chi, K.-M. Hoe, N. Balasubramanian, G. S. Samudra, and Y.-C. Yeo, J. Electrochem. Soc. **155**(3), H151 (2008).
[10]R. T.-P. Lee, T.-Y. Liow, K.-M. Tan, A. E.-J. Lim, A. T.-Y. Koh, M. Zhu, G.-Q. Lo, G. S. Samudra, D. Z. Chi, and Y.-C. Yeo, IEEE Electron Device Lett. **29**(4), 382 (2008).
[11]R. T. P. Lee, A. E.-J. Lim, K.-M. Tan, T.-Y. Liow, G.-Q. Lo, G. S. Samudra, D. Z. Chi, and Y.-C. Yeo, IEEE Electron Device Lett. **28**, 164 (2007).
[12]M. Sinha, R. T.-P. Lee, E. F. Chor, and Y. C. Yeo, IEEE Trans. Electron Devices **57**(6), 1279 (2010).
[13]M. Sinha, R. T.-P. Lee, E. F. Chor, and Y. C. Yeo, IEEE Electron Device Lett. **30**(12), 1278 (2009).
[14]M. Sinha, R. T. P. Lee, K.-M. Tan, G.-Q Lo, E.-F. Chor, and Y.-C. Yeo, IEEE Electron Device Lett. **30**, 85 (2009).
[15]M. Sinha, E.-F. Chor, and Y.-C. Yeo, Appl. Phys. Lett. **92**, 222114 (2008).
[16]S.-M. Koh, M. Sinha, Y. Tong, H.-C. Chin. W.-W. Fang, X. Zhang, C.-M. Ng, G. S. Samudra, and Y.-C. Yeo, Int. Semicond. Device Res. Symp., (College Park MD, Dec. 9–11, 2009).
[17]E. Alptekin and M. C. Ozturk, IEEE Electron Device Lett. **30**(12), 1272 (2009).
[18]R. T.-P. Lee, A. E.-J. Lim, K.-M. Tan, T.-Y. Liow, D. Z. Chi, and Y.-C. Yeo, IEEE Electron Device Lett. **30**(5), 472 (2009).
[19]E. Alptekin, M. C. Ozturk, and V. Misra, IEEE Electron Device Lett. **30**(4), 331 (2009).
[20]H.-S. Wong, L. Chan, G. Samudra, and Y.-C. Yeo, Appl. Phys. Lett. **93**(7), 0721031 (2008).
[21]H.-S. Wong, L. Chan, G. Samudra, and Y.-C. Yeo, IEEE Electron Device Lett. **28**(12), 1102 (2007).
[22]Q. T. Zhao, U. Breuer, E. Rije, S. Lenk, and S. Mantl, Appl. Phys. Lett. **86**(6), 0621081 (2005).
[23]C. Ortolland, E. Rosseel, N. Horiguchi, C. Kerner, S. Mertens, J. Kittl, E. Verleysen, H. Bender, W. Vandervost, A. Lauwers, P. P. Absil, S. Biesemans, S. Muthukrishnan, S. Srinivasan, A. J. Mayur, R. Schreutelkamp, and T. Hoffmann, Tech. Dig. – Int. Electron Devices Meet. **23** (2009).
[24]A. Steegen, R. Mo, R. Mann, M.-C. Sun, M. Eller, G. Leake, D. Vietzke, A. Tilke, F. Guarin, A. Fischer, T. Pompl, G. Massey, A. Vayshenker, W.L. Tan, A. Ebert, W. Lin, W. Gao, J. Lian, J.-P. Kim, P. Wrschka, J.-H. Yang, A. Ajmera, R. Knoefler, Y.-W. The, F. Jamin, J. E. Park, K. Hooper, C. Griffin, P. Nguyen, V. Klee, V. Ku, C. Baiocco, G. Johnson, L. Tai, J. Benedict, S. Scheer, H. Zhuang, V. Ramanchandran, G. Matusiewicz, Y.-H. Lin, Y. K. Siew, F. Zhang, L. S. Leong, S. L. Liew, K. C. Park, K.-W. Lee, D. H. Hong; S.-M. Choi, E. Kaltalioglu, S. O. Kim, M. Naujok, M. Sherony, A. Cowley, A. Thomas, J. Sudijohno, T. Schiml, J.-H. Ku, and I. Yang, Tech. Dig. – Int. Electron Devices Meet. **64** (2005).
[25]M. Tsuchiaki, K. Ohuchi, and C. Hongo, J. Appl. Phys. **43**, 5166 (2004).
[26]D. Z. Chi, D. Mangelinck, J. Y. Dai, S. K. Lahiri, K. L. Pey, and C. S. Ho, Appl. Phys. Lett. **76**, 3385 (2000).
[27]T. Yamaguchi, K. Kashihara, T. Okudaira, T. Tsutsumi, K. Maekawa, N. Murata, J. Tsuchimoto, K. Asai, and M. Yoneda, IEEE Trans. Electron Devices **56**(2), 206 (2009).
[28]D. Deduytsche, C. Detavernier, R. L. V. Meirhaeghe, and C. Lavoie, J. Appl. Phys. **98**, 1 (2005).
[29]V. Teodorescu, L. Nistor, H. Bender, A. Steegen, A. Lauwers, K. Maex, and J. V. Landuyt, J. Appl. Phys. **90**, 167 (2001).
[30]J. Mileham, V. Le, S. Shetty, J. Hebb, Y. Wang, D. Owen, R. Binder, R. Giedigkeit, S. Waidmann, I. Richter, K. Dittmar, H. Prinz, and M. Weisheit, in *18th IEEE Int. Conf. on Advanced Thermal Processing of Semiconductors*, pp. 130–135 (2010).
[31]Y.-W. Chen, N.-T Ho, J. Lai, T. C. Tsai, C. C. Huang, J. Y. Wu, B. Ng, A. J. Mayur, A. Tang, S. Muthukrishnan, J. Zelenko, H. Yang, in *17th IEEE Int. Conf. on Advanced Thermal Processing of Semiconductors*, pp. 213–216 (2009).
[32]B. Adams, D. Jennings, K. Ma, A. J. Mayur, S. Moffatt, S. G. Nagy, and V. Parihar, in *15th IEEE Int. Conf. on Advanced Thermal Processing of Semiconductors*, pp. 155–160 (2007).
[33]Y. Setiawan, P. S. Lee, K. L. Pey, X. C. Wang, G. C. Lim, and B. L. Tan, Appl. Phys. Lett. **90**, 073108 (2007).
[34]Y. Setiawan, P. S. Lee, K. L. Pey, X. C. Wang, and G. C. Lim, Appl. Phys. Lett. **88**, 113108 (2006).
[35]J.-S. Luo, W.-T. Lin, C. Y. Chang, and W. C. Tsai, Mat. Chem. Phys. **54**, 160 (1998).
[36]B. Weber, K. Gärtner, A. Witzmann, and C. Kaschner, Appl. Surf. Sci. **54**, 381 (1992).
[37]P. Baeri, M. G. Grimaldi, F. Priolo, A. G. Cullis, and N. G. Chew, J. Appl. Phys. **66**, 861 (1989).
[38]M. A. Harith, J. P. Zhang, P. Baeri, E. Rimini, and G. Celotti, J. Appl. Phys. **57**, 4560 (1985).
[39]G. G. Bentini, M. Servidori, C. Cohen, R. Nipoti and A. V. Drigo, J. Appl. Phys. **53**, 1525 (1982).
[40]J. F. Ziegler and J. P. Bierack, see http://www.srim.org for "Stopping and Range of Ions in Matter."
[41]R. K. Singh and J. Narayan, Mater. Sci. Eng. B **3**, 217 (1989).
[42]O. Krause, H. Ryssel, and P. Pichler, J. Appl. Phys. **91**, 5645 (2002).
[43]David R. Lide, *CRC Handbook of Chemistry and Physics*, 84th ed., (CRC, Boca Raton, FL, 2003), pp. 4-132.
[44]S.-D. Kim, C.-M Park and J. C. S. Woo, Solid-State Electron. **49**, 131 (2005).
[45]M. F. V. Allmen and S. S. Lau, in *Laser Annealing of Semiconductors*, edited by J. M. Poate and J. W. Mayer (Academic, New York, 1982), p. 450.
[46]T. P. Norlan, R. Sinclair, and R. Beyers, J. Appl. Phys. **71**, 720 (1992).
[47]C. Lavoie, F. M. d'Heurle, C. Detavernier, and C. Cabral, Jr., Microelectron. Eng. **70**, 144 (2003).
[48]S. M. Sze, *Physics of Semiconductor Devices*, 2nd ed. (Wiley, New York, 1981).
[49]T. Yamauchi, Y. Nishi, Y. Tsuchiya, A. Kinoshita, J. Koga, and K. Kato, Tech. Dig. – Int. Electron Devices Meet. **963**, (2007).
[50]J. F. Gibbons and T. W. Sigmon, in *Laser Annealing of Semiconductors*, edited by J. M. Poate and J. W. Mayer (Academic, New York, 1982), p. 369.
[51]S. U. Campisano, G. Foti, P. Baeri, M. G. Grimaldi, and E. Rimini, Appl. Phys. Lett. **37**, 719 (1980).
[52]C.-D. Lien, F. C. T. So, and M.-A. Nicolet, IEEE Trans. Electron Devices **ED-31**(10), 1502 (1984).
[53]R. L. Van Meirhaeghe, W. H. Laflere, and F. Cardon, J. Appl. Phys. **76**(1), 403 (1994).
[54]P. Hadizad, A. S. Yapsir, T.-M. Lu, and J. C. Corelli, Nucl. Instrum. Methods Phys. Res. **B19/20**, 431, (1987).